Generation of Linear Frequency-Modulated Waveforms by a Frequency-Sweeping Optoelectronic Oscillator

Pei Zhou, *Student Member, IEEE*, Fangzheng Zhang, *Member, IEEE*, and Shilong Pan, *Senior Member, IEEE, Senior Member, OSA*

***Abstract*—In this paper, a simple scheme for linear frequency-modulated (LFM) waveform generation based on a frequency-sweeping optoelectronic oscillator is proposed and demonstrated. The OEO is built up with an optically injected semiconductor laser and the oscillation frequency can be tuned by adjusting the optical injection strength. By applying an injection strength controller in the OEO for rapid frequency sweeping, an LFM microwave waveform can be generated. When the sweep period of the output frequency matches with the round-trip time of the OEO cavity, signal quality of the generated LFM waveform can be significantly enhanced by the high Q optoelectronic oscillation. In the experiment, an LFM signal with a bandwidth as large as 7 GHz, a chirp rate reaching 0.18 GHz/ns, and a time-bandwidth product (TBWP) up to 2804.2 is generated. The corresponding electrical spectrum is a frequency comb with a contrast as high as 47 dB. Based on this system, an improved scheme for extending the frequency and bandwidth of the generated LFM signal is proposed by employing a polarization modulator to implement microwave photonic frequency multiplication. With this method, an LFM waveform with a TBWP as large as 13839.1 (bandwidth 15.6 GHz; temporal period 887.12 ns) is obtained.**

***Index Terms*—Linear frequency modulation, microwave photonics, optical injection, optoelectronic oscillator, semiconductor laser.**

I. Introduction

LINEAR frequency-modulated (LFM) waveform generation has been considered as a key technique in modern radar systems [1]–[4], because LFM waveforms have been widely employed to enhance both the radar range resolution and detecting distance. Conventionally, LFM waveforms are produced electrically via a voltage-controlled oscillator (VCO) with a linearly ramping control voltage or a direct digital synthesizer (DDS). However, due to the limitation of current electronic devices, an electrically produced LFM waveform normally possess a small bandwidth and a low central frequency. Therefore, to take advantage of the broadband and high-speed characteristics offered by photonics, many photonic-based methods have been proposed to generate LFM waveforms. These methods can be classified into two main categories: (i) spectral shaping together with wavelength-to-time mapping (WTTM) [5]–[7] and (ii) external phase-modulation [8] or polarization modulation [9]. In the first kind of method, an optical spectral shaper is employed to manipulate the optical spectrum of a mode-locked laser. Then, WTTM is performed to produce a broadband LFM waveform after propagating through a dispersive element. However, the generated LFM waveform usually suffers from a poor tunability as well as a small temporal duration, which can hardly meet the requirements in many radar applications. For the second kind of method, the main drawback is that the achievable time-bandwidth product (TBWP) is normally no more than 10, which is limited by the small modulation index of the current modulator. Recently, researchers proposed to enlarge the modulation depth and the resultant TBWP by recirculating phase-modulation [8] or splitting the parabolic driving electrical signal [9], but the TBWP is still limited in both cases. What's more, the use of a high-speed microwave arbitrary waveform generator (AWG) would lead to a significant increase in system complexity and cost.

In Ref. [10], we proposed a photonic scheme to generate LFM waveforms with a large TBWP by an optically injected semiconductor laser. By introducing a low-speed electrical signal to manipulate the dynamical injection strength of a semiconductor laser, LFM waveforms with TBWPs as large as 1.2×10^5 (10–22 GHz, 10 μs) are generated. The major drawback of the generated photonic microwave signal is its poor quality and it has a large linewidth of 1–10 MHz. To address this problem, optoelectronic feedback structure is used to stabilize the generated microwave signal through optically injected semiconductor lasers [11]–[14]. In Ref. [12], sinusoidal frequency-modulated (SFM) microwave waveform generation has been demonstrated by using an optically injected semiconductor laser and optoelectronic feedback stabilization. In this method, the electrical signal is applied to a high-speed Mach-Zehnder modulator (MZM) to form a feedback loop. A SFM signal with a bandwidth of

Manuscript received March 5, 2018; revised June 7, 2018; accepted July 6, 2018. Date of publication July 10, 2018; date of current version July 19, 2018. This work was supported in part by the National Natural Science Foundation of China under Grant 61527820, in part by the Natural Science Foundation of Jiangsu Province under Grant SBK2018030017, in part by the Fundamental Research Funds for the Central Universities under Grant NS2018028, and in part by the China Scholarship Council (CSC) program. *(Corresponding authors: Fangzheng Zhang and Shilong Pan.)*

The authors are with the Key Laboratory of Radar Imaging and Microwave Photonics, Ministry of Education, Nanjing University of Aeronautics and Astronautics, Nanjing 210016, China (e-mail: zhou_pei@nuaa.edu.cn; zhangfangzheng@nuaa.edu.cn; pans@ieee.org).

Color versions of one or more of the figures in this paper are available online at http://ieeexplore.ieee.org.

Digital Object Identifier 10.1109/JLT.2018.2854713

7.7 GHz and a chirp rate of 0.42 GHz/ns is obtained. However, the use of high-speed MZM not only increases the system cost, but also limits the available frequency range of the generated signal. In the experiment, the highest frequency of the achieved SFM signal is around 18 GHz. Accordingly, bandwidth requirement of the MZM is no less than 18 GHz.

Meanwhile, it has been demonstrated that optoelectronic oscillator (OEO) is a promising method to generate frequency-tunable and high-quality microwave signals [15], [16]. However, when the central frequency of an OEO is tuned to achieve frequency sweeping, oscillation has to be established from thermal noise at every new frequency. Such non-stationary operation, leading to a temporally varying distribution of energy between the eigen modes of the OEO cavity, would limit the frequency sweep rate, and result in degraded performance, such as linewidth broadening, phase discontinuity and limited tuning range. Therefore, the study on a frequency scanning OEO for LFM waveform generation has been rarely reported.

In this paper, a simple approach for LFM waveform generation based on a frequency-sweeping OEO is proposed. The OEO is built up with an optically injected semiconductor laser, and its frequency tunability is achieved by adjusting the optical injection strength. In the proposed system, an "injection strength controller" is introduced to achieve rapid tuning of the OEO, and an LFM microwave waveform is thus generated. When the sweep period of the output frequency matches with the round-trip time of the OEO cavity, which produces a quasi-stationary mode of operation, and signal quality of the generated LFM waveform can be significantly enhanced by the high Q optoelectronic oscillation. In the experiment, an LFM signal with a sweep range as large as 7 GHz, a tuning rate reaching 0.18 GHz/ns, and a time-bandwidth product (TBWP) up to 2804.2 is generated. A frequency comb contrast of 47 dB is also observed in the spectrum. Besides, feasibility of tuning the bandwidth, temporal period and frequency band of the generated LFM waveform is also demonstrated. Furthermore, in order to achieve a higher frequency and a larger bandwidth, an improved scheme is further proposed and demonstrated, where a polarization modulator (PolM) is employed. Such an approach achieves frequency multiplication of the generated LFM signal since the PolM can realize frequency-multiplying modulation. Experimental results show that LFM waveform with a bandwidth up to 15.6 GHz can be obtained. Meanwhile, the resultant TBWP is multiplied accordingly.

II. Principle

The basic schematic diagram of the proposed photonic LFM waveform generator using a tunable OEO is shown in Fig. 1. In the system, a single-mode semiconductor laser is served as the slave laser. Under continuous-wave optical injection, period-one (P1) dynamics can be excited by undamping the relaxation resonance of semiconductor lasers. The output intensity of the injected slave laser shows self-sustained intensity oscillation [17]–[19]. Its optical spectrum exhibits highly asymmetric double sideband modulation and the modulation frequency equals to the P1 frequency f_o. A microwave signal can be obtained

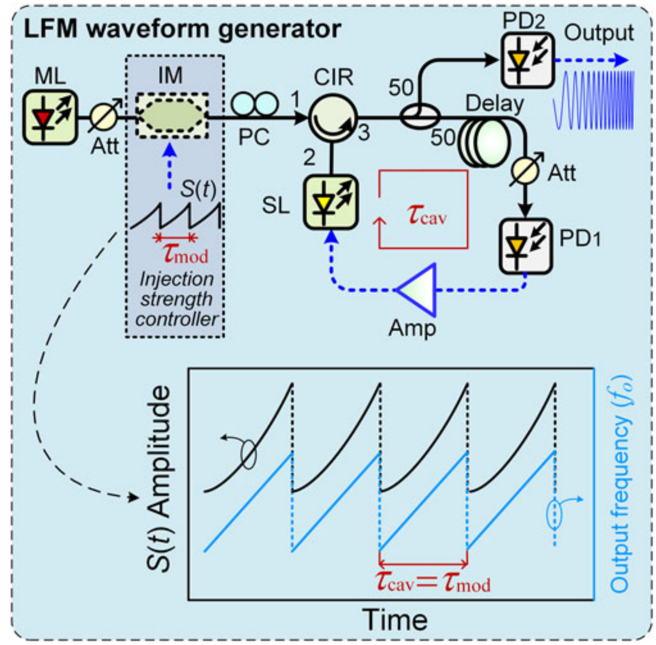

Fig. 1. Schematic diagram of the proposed photonic LFM waveform generator. ML: master laser, Att: optical attenuator, IM: intensity modulator, $S(t)$: control signal, PC: polarization controller, SL: slave laser, CIR: optical circulator, PD: photodetector, Amp: microwave amplifier.

with a frequency of f_o after photodetection. By simply varying the optical injection strength ξ and the detuning frequency f_i, the obtained microwave frequency is able to be varied from a few to over one hundred gigahertz. Here, f_i equals to the difference between the master and free-running slave laser, and the injection strength ξ is defined as $\xi = \sqrt{P_{in}/P_{sl}}$, where P_{in} and P_{sl} is the power of the injected optical signal and the free-running slave laser. Although broadly tunable, this generated signal has a large linewidth of 1–10 MHz, which mainly arises from the intrinsic laser noise. To narrow the linewidth, an OEO is constructed by adding an optoelectronic feedback loop. In the setup, a portion of the optical output after the optical circulator (lower branch) is delayed by a section of fiber, and then sent to a photodetector (PD). Afterwards, the detected microwave signal is amplified and fed back to modulate the slave laser. The microwave output can be obtained from the upper branch by using another PD. Thus, a tunable optoelectronic oscillator is formed and frequency tuning is achieved through controlling f_i and/or ξ.

For a given detuning frequency f_i, the P1 frequency f_o would increase approximately linearly with increasing injection strength ξ. Such property has been verified both numerically and experimentally in previous reports [19], [20]. Owing to the fast dynamical behavior of semiconductor lasers, typically a sub-nanosecond time scale, the instantaneous frequency of obtained microwave signal can be controlled by introducing an "injection strength controller". As a result, if the control signal $S(t)$ is set to be a quasi-sawtooth wave, the injected optical signal should have a linearly increased amplitude. Hence, the resultant microwave frequency would also increase linearly with time, namely, an LFM waveform is obtained. As depicted in the

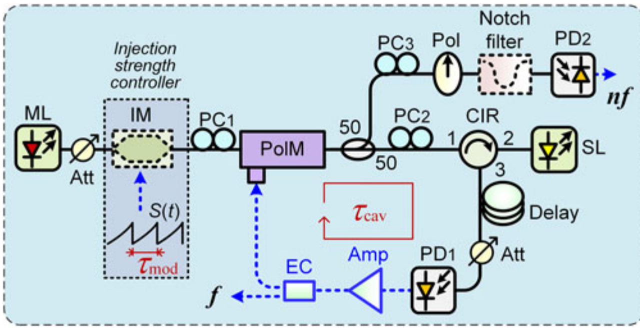

Fig. 2. Proposed frequency-multiplied LFM waveform generation scheme. PolM: polarization modulator, Pol: polarizer, EC: electrical coupler.

lower part of Fig. 1, to achieve the phase noise improvement of the generated LFM waveform by optoelectronic feedback, the period of control signal $S(t)$ (i.e., τ_{mod}) should be carefully tuned to match with the round-trip time of the OEO cavity (i.e., τ_{cav}). Under this condition (i.e., $\tau_{\mathrm{mod}} = \tau_{\mathrm{cav}}$), a quasi-stationary mode of operation is produced, and phase noise reduction for the generated LFM signal is possible. Because, for one thing, the optoelectronic feedback cavity sustains a sequence of eigen modes spaced by $1/\tau_{\mathrm{cav}}$. On the other hand, a specific microwave mode passes through the OEO cavity and return to modulate the slave laser at the exact moment when the injection induced P1 oscillation is at the same spectral position, and optoelectronic oscillation does not need to be established from thermal noise. That is to say, the OEO cavity stores an entire frequency sweep in the delay line. Such operation principle is also known as Fourier Domain Mode Locking (FDML), which is first proposed by R. Huber *et al.* to realize a frequency-sweeping fiber laser in 2006 [21]. In ideal circumstances, the OEO outputs a signal with its frequency swept with a step equaling to the cavity repetition rate and a fixed phase relationship. In this case, LFM waveforms with better phase noise performance can be generated. According to the above principle, the bandwidth, temporal period and frequency band of the generated LFM waveform are controllable. For instance, the bandwidth of the LFM waveform can be enlarged by setting a larger amplitude of $S(t)$.

Similar to the basic approach, an improved scheme for frequency-multiplied LFM waveform generation is proposed as shown in Fig. 2, where a polarization modulator (PolM) is employed in the OEO loop. In this case, the detected microwave signal is feedback to drive the PolM instead of the slave laser to form an optoelectronic feedback cavity. The PolM is a special phase modulator that can support both transverse-electric and transverse-magnetic modes with however opposite phase modulation indices [22]. Compared with a conventional Mach-Zehnder modulator (MZM), a PolM has superiorities in realizing the frequency-multiplied OEO [23]. The optical output of the PolM is split into two branches. In the lower branch, the polarization of the injection light is adjusted to match with that of the slave laser. In the upper branch, a portion of the optical signal after the PolM is sent to a PC and a polarizer, and fundamental-frequency or frequency-doubling intensity modulation can be easily realized by adjusting the PC [24]. Furthermore, if an optical notch filter is used to remove some undesirable optical sidebands, frequency-quadrupling [25] or frequency-sextupling [26] intensity modulation is also achievable. Therefore, frequency-multiplied LFM waveform can be obtained after the PD2 while maintaining the oscillation of the fundamental-frequency LFM waveform in the OEO loop.

III. Experimental Demonstration

Based on the above principle, we experimentally verify the LFM waveform generation scheme by a tunable OEO as well as the improved frequency-multiplied scheme as shown in Figs. 1 and 2.

A. Basic Approach

For the basic scheme, no high-speed modulator is needed. The master laser is a tunable laser and its power can be tuned by an optical attenuator. A distributed-feedback (DFB) laser biased at $\sim$5 times its threshold current of 31.7 mA is used as the slave laser. Its free-running power and wavelength is 4.6 dBm and 1553.253 nm, respectively. A PC aligns the polarization of the injected optical signal to match with that of slave laser to maximize the injection efficiency. The “injection strength controller” includes a 10-Gb/s MZM and an electrical control signal from a 120-MHz AWG (Agilent 81150A). Both PDs have a bandwidth of 18 GHz and a responsivity of 0.85 A/W. The microwave amplifier has a gain of $\sim$ 30 dB. The generated LFM waveforms are monitored by an electrical spectrum analyzer (ESA, R&S FSV40, and FSWP50) and a real-time oscilloscope (Keysight DSO-X 92504A).

First of all, the control signal $S(t)$ is switched off and the optical injection strength is controlled by an optical attenuator. The master-slave detuning frequency is set to 2.7 GHz. In Fig. 3(a), the slave laser is optically injected at $(f_{\mathrm{i}}, \xi) = (2.7\,\mathrm{GHz}, 0.42)$ which leads to a P1 oscillation frequency of $f_{\mathrm{o}} = 15.7\,\mathrm{GHz}$. As can be seen in Fig. 3(a), the optical spectrum consists of equally spaced sidebands that are separated by 15.7 GHz. After optical-to-electrical conversion, the optical components generate a beating signal at 15.7 GHz, as shown by the red curve in Fig. 3(b). Due to the intrinsic laser noise, a relatively large 3-dB linewidth of 0.8 MHz is observed. After introducing an optoelectronic feedback loop with an effective cavity length of $\sim$7.66 m, i.e., the OEO is enabled, the microwave linewidth is significantly reduced to $\sim$8.5 kHz, as shown by the black curve in Fig. 3(b). The output frequency as a function of the injection strength ξ is meaured and shown in Fig. 3(c). It is observed that the output microwave frequency increases linearly as ξ increases. The single-sideband (SSB) phase noise of the generated microwave signal with optoelectronic feedback at different frequenies are measured and shown in Fig. 3(c), where the SSB phase noises is between -112.9 and -104.3 dBc/Hz @ 1 MHz offset.

Next, the “injection strength controller” is enabled, and the 26.095-MHz control signal $S(t)$ has an amplitude of $\sim$1 V. Here, the profile of $S(t)$ is made to compensate for the nonlinearity in amplitude transfer function of the system [10]. The modulated

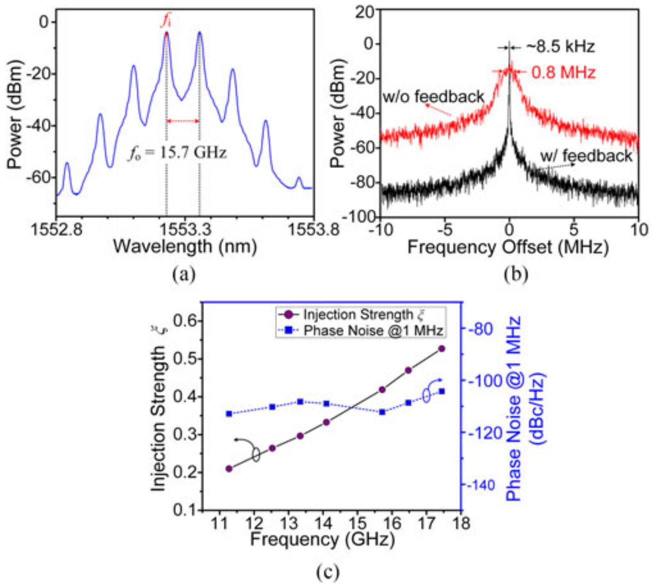

Fig. 3. (a) Optical spectrum and (b) electrical spectrum when (f_i, ξ) equals to (2.7 GHz, 0.42), (c) output frequency as a function of the injection strength and measured phase noise @ 1 MHz for different frequencies.

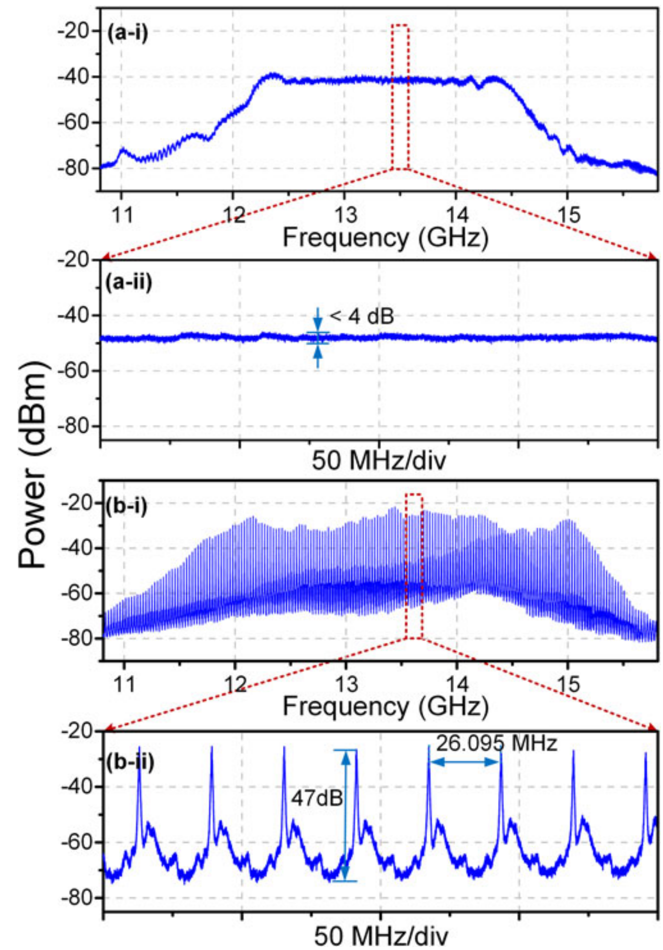

Fig. 4. Measured electrical spectra of generated LFM signals (a) without (b) with optoelectronic feedback. (i) Span: 5GHz, RBW: 100 kHz; (ii) span: 200 MHz, RBW: 20 kHz.

frequency of 26.095 MHz is carefully set to equal to the reciprocal of the cavity round-trip time τ_{cav}, and $\tau_{\text{mod}} = \tau_{\text{cav}}$ is satisfied. Fig. 4 shows the measured electrical spectra of the generated LFM waveforms (a) without and (b) with optoelectronic feedback. The ideal spectrum of a periodical LFM waveform is a microwave frequency comb spaced by $1/\tau_{\text{mod}}$. When the optoelectronic feedback is not applied, the spectrum in Fig. 4(a) suffers from the large phase noise and uncorrelated phase relationship, resulting in a low comb contrast R of no more than 4 dB. In contrast, when the delay-matched optoelectronic feedback loop is employed, i.e., the optoelectronic oscillator is enabled, a series of sharp frequency comb components spaced by $1/\tau_{\text{cav}}$ are obtained, as shown in Fig. 4(b). Due to the fixed phase relationship and reduced phase noise by the high Q optoelectronic oscillation, the comb contrast R is effectively increased to 47 dB. Compared with the spectrum in Fig. 4(a), a 43-dB improvement of the comb contrast R is achieved with optoelectronic feedback. It should be noted that, some residual sidebands are observed in Fig. 4(b-ii), which is mainly caused by frequency jitters of the P1 oscillation frequency. When the modulation frequency is fine-tuned to match the mode spacing, the noisy sidebands can be reduced and minimized.

The waveform of the generated LFM signal with a temporal period of 38.32 ns is shown in Fig. 5(a). The detailed waveforms at the start and end of a period with a duration of 1 ns are also displayed in the insets of Fig. 5(a). It should be noted that, the amplitude of the generated LFM waveform shows some fluctuation as the frequency changes, which is attributed to the uneven frequency response of the P1 oscillation and the devices (e.g., the electrical amplifier) in the optoelectronic feedback cavity [19]. The instantaneous frequency of the LFM waveform is calculated based on the short-time Fourier transform (STFT). As indicated in Fig. 5(b), the generated LFM waveform has a bandwidth of 3.3 GHz (11.9–15.2 GHz). Therefore, the generated LFM waveform has a TBWP of 126.5. In order to verify the pulse compression ability, the autocorrelation curve is calculated and shown in Fig. 4(c), where the full width at half maximum (FWHM) of the autocorrelation peak is measured to be 0.4 ns. The pulse compression ratio is calculated to be 95.8, which is smaller than the theoretical value of 104.9. To enhance the pulse compression ratio, one can improve the amplitude flatness in the generated waveform by using power limiting techniques [27], [28].

For the proposed scheme, the bandwidth, or the frequency sweeping range of the generated LFM waveform can be separately tuned. As shown in Fig. 6(a), when the amplitude of $S(t)$ is adjusted to ~2.2 V, frequency sweep range of the obtained LFM waveform is enlarged to 7 GHz (10.7–17.7 GHz). This indicates that the sweep rate is 0.18 GHz/ns and the TBWP is 268.2. Besides, the feasibility of tuning the temporal period of the generated LFM waveform is demonstrated. By using a longer delay in the optoelectronic feedback loop, the cavity round-trip time τ_{cav} is increased to 849.76 ns, and the tuning speed of $S(t)$ is correspondingly adjusted to 1.1768 MHz to match with $1/\tau_{\text{cav}}$. At the output, an LFM waveform with a period of 849.76 ns and

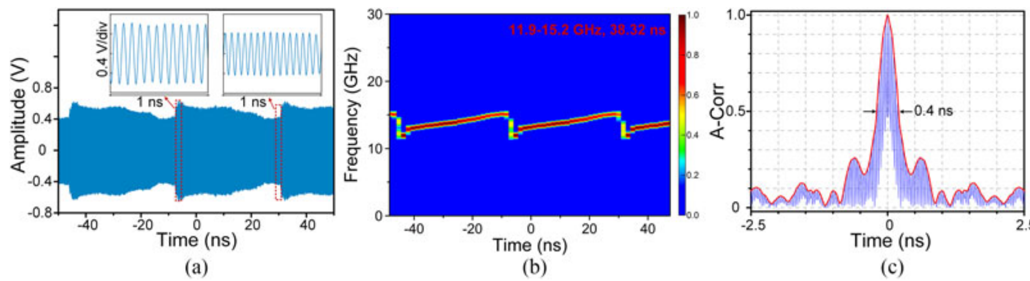

Fig. 5. (a) Measured waveform of the produced LFM signal (Insets: enlarged views of 1-ns waveform), (b) calculated frequency-to-time relation, (c) autocorrelation curve.

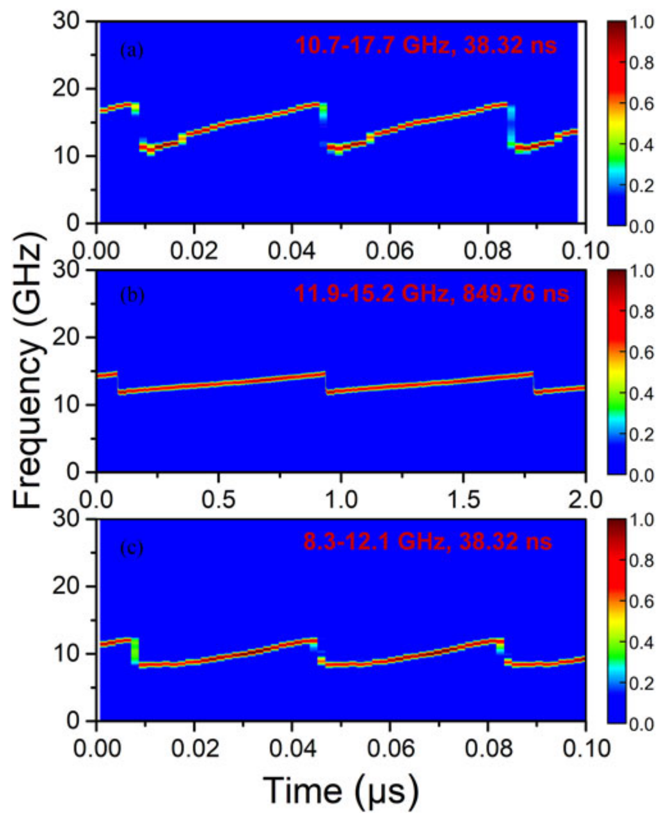

Fig. 6. Calculated frequency-to-time relations of the obtained LFM waveforms with (a) different bandwidth, (b) different temporal period, and (c) different frequency band.

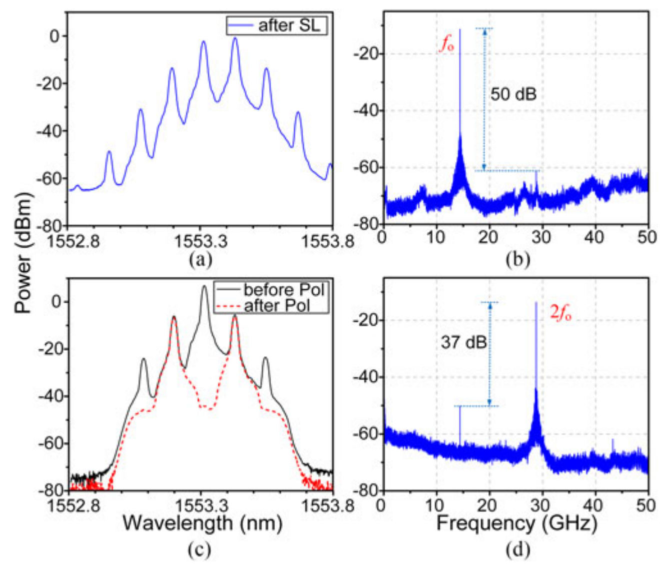

Fig. 7. Generation of 14.4- and 28.8-GHz signals using the PolM-based OEO. (a) Optical and (b) electrical spectrum (RBW: 3 MHz) of the in-loop fundamental-frequency signal; (c) optical and (d) electrical spectrum (RBW: 3 MHz) of the out-loop frequency-doubled signal.

a bandwidth of 3.3 GHz (11.9-15.2 GHz) is obtained. Fig. 6(b) depicts its instantaneous frequency. The LFM waveform has a large TBWP of about 2804.2. Furthermore, by changing the master-slave detuning frequency f_{i} from $\sim$2.7 GHz to $\sim$0.4 GHz, an LFM signal covering a frequency range of 8.3-12.1 GHz with a temporal period of 38.32 ns is obtained, as shown in Fig. 6(c).

B. Improved Approach

For a given slave laser with a fixed detuning frequency f_{i}, the largest bandwidth of the generated LFM waveform based on the above approach is no more than its achievable P1 frequency range, which is typically around 10 GHz [17]–[19]. In our experiment, due to the limited optical power of the master laser and the large insertion loss of the intensity modulator, the largest bandwidth is limited to around 7 GHz. To overcome this frequency and bandwidth limitation, an improved scheme is built up based on the setup in Fig. 2. In the experiment, the PolM (Verswave Technologies) and PD2 have a bandwidth of 40 and 50 GHz, respectively. Firstly, the "injection strength controller" is disabled, i.e., $S(t)$ is not applied. The PolM-based OEO is operated at the single-frequency oscillation state and its oscillation frequency (equals to P1 frequency) can also be tuned by adjusting the optical injection strength via an optical attenuator. Fig. 7 shows the measured optical and electrical spectra when the P1 frequency (f_{o}) equals to 14.4 GHz. Fig. 7(a) is the optical spectrum of P1 oscillation measured at port 3 of the optical circulator. At the output of the electrical coupler, a fundamental-frequency signal of 14.4 GHz is obtained with its spectrum shown in Fig. 7(b). As can be seen, power of the 14.4-GHz signal is 50 dB higher than its second harmonic frequency. Meanwhile, a frequency-doubled signal at 28.8 GHz is generated after PD2. For ease of comparison, Fig. 7(c) shows the optical spectra before (black curve) and after (red curve) the Pol. Before the Pol, the optical spectrum is the result of polarization modulation, having an

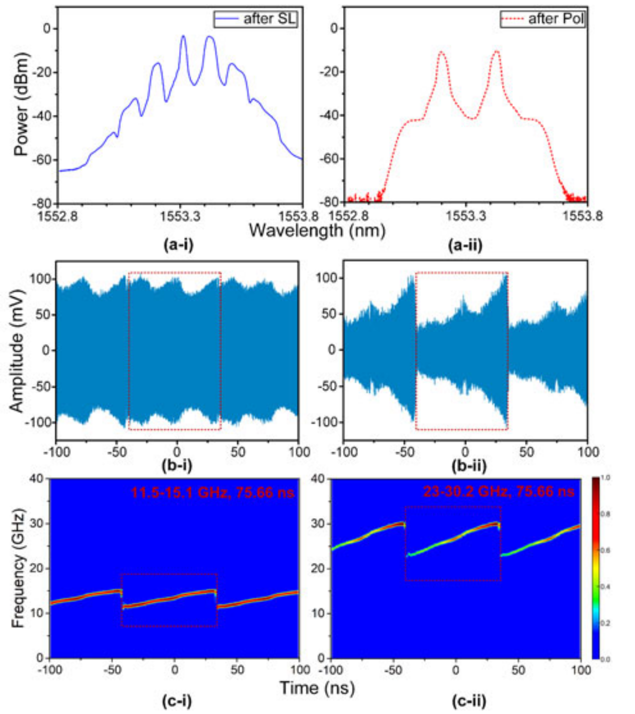

Fig. 8. (a) Measured optical spectra, (b) measured temporal waveforms and (c) calculated frequency-to-time relations for (i) in-loop fundamental-frequency and (ii) out-loop frequency-doubled LFM signals.

optical carrier with two first-order sidebands. After the Pol, the optical spectrum is the result of equivalent intensity modulation operating at the minimum transmission point (MITP) by properly setting PC3, and the optical carrier is suppressed by about 51 dB compared with the spectrum before the Pol. Correspondingly, power of the generated 28.8-GHz electrical signal is 37 dB higher than its fundamental-frequency component, as shown in Fig. 7(d).

Then, the "injection strength controller" is enabled to generate LFM waveforms. A 13.216-MHz control signal $S(t)$ which has a quasi-sawtooth profile and an amplitude of $\sim$1.5 V is applied to the MZM to control the injection strength. Here, the frequency of $S(t)$ is also set to match with the cavity round-trip time. Both the fundamental-frequency and frequency-doubled LFM waveforms are generated. In Fig. 8(a), the optical spectra (i) at port 3 of the optical circulator inside the OEO cavity and (ii) after Pol outside the OEO loop are presented, where the results resemble those in Fig. 7. In Fig. 8(b), both (i) fundamental-frequency and (ii) frequency-doubled LFM waveforms have a temporal period of 75.66 ns. Different from Fig. 8(b-i), the waveform in Fig. 8(b-ii) shows approximately increasing amplitude in a period, which is attributed to the quasi-sawtooth modulation of the incoming optical carrier before the PolM. After optical-to-electrical conversion, the obtained LFM waveform would also have an approximately increasing amplitude within a period. This uneven amplitude can be solved by using either electrical or optical power limiting techniques. For instance, in the photonic LFM waveform generation scheme in [27], an optical limiting amplifier (LMA) [28] is used to compensate for the amplitude

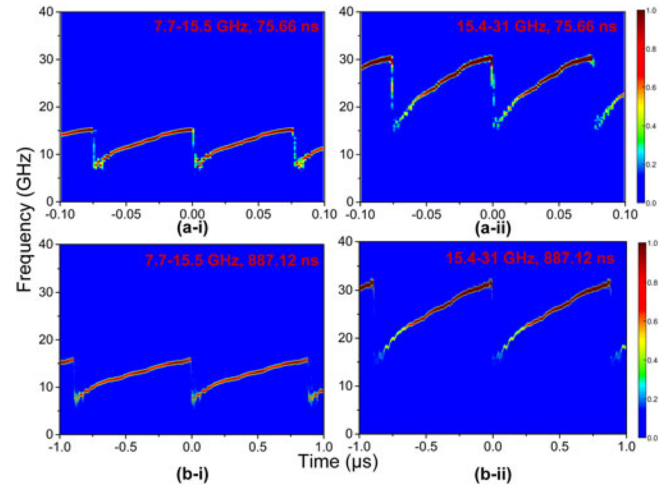

Fig. 9. Calculated frequency-to-time relations of the obtained LFM waveforms with (a) different bandwidth, (b) different temporal period for (i) in-loop fundamental-frequency and (ii) out-loop frequency-doubled LFM signals.

fluctuations. Fig. 8(c) shows the calculated frequency-to-time relations via STFT analysis. As can be seen in Fig. 8(c-i), the in-loop fundamental-frequency LFM waveform covers a frequency range of 11.5–15.1 GHz, corresponding to a bandwidth of 3.6 GHz. Accordingly, in Fig. 8(c-ii), the frequency-doubled LFM signal covers 23–30.2 GHz with a bandwidth of 7.2 GHz.

Compared with the results in Fig. 8, both bandwidth and temporal period of the generated LFM waveforms can be boosted. Fig. 9 shows the STFT analysis of the generated signals with an enlarged bandwidth and temporal period. As shown in Fig. 9(a-i), bandwidth of the generated LFM waveform is enlarged to 7.8 GHz (7.7–15.5 GHz) by adjusting the amplitude of $S(t)$ to $\sim$2 V. Meanwhile, bandwidth of the frequency-doubled LFM waveform is enlarged to 15.6 GHz (15.4–31 GHz) in Fig. 9(a-ii), corresponding to a sweep rate of 0.206 GHz/ns. Then, a longer delay is used in the optoelectronic feedback loop and the tuning speed of $S(t)$ is slowed down to 1.127 MHz to match with $1/\tau_{cav}$. As shown in Fig. 9(b), the temporal period of the generated LFM waveforms is increased to 887.12 ns while the frequency coverage is maintained for both (i) fundamental-frequency and (ii) frequency-doubled LFM signals. Therefore, the frequency-doubled LFM signal has a large TBWP of about 13839.1 (15.4-31 GHz, 887.12 ns), as depicted in Fig. 9(b-ii).

Furthermore, if an optical notch filter is used to remove some undesirable optical sidebands, frequency-quadrupling [25] or frequency-sextupling [26] intensity modulation is also achievable. Therefore, bandwidth and frequency coverage of the generated LFM waveforms can be further enlarged. For instance, in order to generate frequency-quadrupled LFM waveforms, the PolM-based IM (PolM + PC3 + Pol) is operating at the maximum transmission point (MATP) rather than MITP. In this case, the optical signal consists of an optical carrier and two second-order sidebands. An optical notch filter is then employed to remove the optical carrier. By beating the two second-order sidebands in PD2, frequency-quadrupled LFM waveforms are achieved. Due to the lack of optical notch filter, the generation

TABLE I
COMPARISON OF FREQUENCY-MODULATED WAVEFORM GENERATION SCHEMES

	Ref. [12]	**Basic Approach**	**Improved Approach**
Waveform Type	SFM	LFM	LFM
Bandwidth	7.7 GHz	7 GHz	15.6 GHz
Chirp Rate [a]	0.42 GHz/ns	0.18 GHz/ns	0.206 GHz/ns
Comb Contrast	45 dB	47 dB	46 dB
TBWP	282.3	2804.2	13839.1
Maximum Frequency	~18 GHz	~18 GHz	~36 GHz
Cost [b]	High	Low	High
Multi-channel Output Ability	No	No	Yes
Multiplication Factor	1	1	2 (4, 6)
Operational Frequency range [c]	Small	Medium	Large

[a]The SFM waveform has both up- and down-chirp in Ref. [12], while the LFM waveform in our work contains only up-chirp. Therefore, for a SFM waveform and LFM waveform with a same bandwidth and temporal period, the SFM waveform naturally possesses a chirp rate which is twice of LFM waveform.

[b]The use of high-speed modulator increases system cost.

[c]Given electrical devices with sufficient frequency, our basic approach has a larger frequency range than Ref. [12]. The possible frequency range can be further enlarged to twice, four times and even six times through PolM-based frequency-multiplication.

of frequency-quadrupled and frequency-sextupled LFM waveforms are not experimentally demonstrated.

Another advantage of the LFM waveform generation scheme using PolM-based OEO is that it can realize flexible multi-port output. At the output of PolM, the upper branch can be split into several paths using a $1 \times N$ splitter. A PC, a polarizer and/or an optical notch filter are inserted in each path. Then, the fundamental-frequency, frequency-doubling, frequency-quadrupling, or frequency-sextupling intensity modulations can be implemented simultaneously. Therefore, the frequency-multiplied LFM waveforms with desired multiplication factors can be generated in each path.

IV. Discussion and Conclusion

Table I presents a comparison of frequency-modulated waveform generation schemes between Ref. [12] and our work. As can be seen, our work (basic approach) has better performance in TBWP, cost, and possible frequency range, while has comparable performance in the rest parameters. Moreover, the improved approach using PolM has better performance in bandwidth, TBWP, maximum frequency, multi-channel output ability, frequency-multiplication factor, and possible frequency coverage. Therefore, we believe that the proposed approaches are more preferred for LFM waveform generation.

In summary, a simple approach for LFM waveform generation based on a frequency-sweeping OEO was proposed and demonstrated. The OEO is built up with an optically injected semiconductor laser, and its frequency tunability is achieved by adjusting the optical injection strength. In the proposed system, an "injection strength controller" is introduced to achieve the rapid tuning of OEO, and an LFM microwave waveform is thus generated. Signal quality of the generated LFM waveform is significantly improved by delay-matched optoelectronic feedback in the OEO. In the experiment, a sweep range as large as 7 GHz, a tuning rate reaching 0.18 GHz/ns and a TBWP up to 2804.2 is obtained. The frequency comb contrast has been improved by 43 dB. Besides, feasibility of adjusting the sweep range, temporal period and frequency band of the produced LFM waveform is also verified. Afterwards, an improved scheme for eliminating the frequency and bandwidth limitation of the obtained LFM waveform is demonstrated based on a polarization modulator. Such an approach achieves the frequency multiplication (up to a factor of six) of the generated LFM signal since the PolM can realize frequency-multiplying modulation. Experimental results show that LFM waveform with a bandwidth up to 15.6 GHz is obtained. Meanwhile, the resultant TBWP is multiplied accordingly. In the experiment, a TBWP as large as 13839.1 (15.4–31 GHz, 887.12 ns) is achieved. Compared with previous approaches, the proposed LFM waveform generator shows superiorities of high frequency, large bandwidth, fast sweeping rate and high spectral purity.

References

[1] M. K. Simon, J. K. Omura, R. A. Scholtz, and B. K. Levitt, *Spread Spectrum Communications Handbook*. New York, NY, USA: McGraw-Hill, 1994.

[2] M. I. Skolnik, *Radar Handbook*, 3rd ed. New York, NY, USA: McGraw-Hill, 2008.

[3] F. Zhang, Q. Guo, and S. Pan, "Photonics-based real-time ultra-high-range-resolution radar with broadband signal generation and processing," *Sci. Rep.*, vol. 7, 2017, Art. no. 13848.

[4] F. Zhang *et al.*, "Photonics-based broadband radar for high-resolution and real-time inverse synthetic aperture imaging," *Opt. Express*, vol. 25, no. 14, pp. 16274–16281, Jul. 2017.

[5] C. Wang and J. P. Yao, "Photonic generation of chirped microwave pulses using superimposed chirped fiber Bragg gratings," *IEEE Photon. Technol. Lett.*, vol. 20, no. 11, pp. 882–884, Jun. 2008.

[6] H. Chi and J. P. Yao, "Chirped RF pulse generation based on optical spectral shaping and wavelength-to-time mapping using a nonlinearly chirped fiber bragg grating," *J. Lightw. Technol.*, vol. 26, no. 10, pp. 1282–1287, May 2008.

[7] F. Zhang, X. Ge, and S. L. Pan, "Background-free pulsed microwave signal generation based on spectral shaping and frequency-to-time mapping," *Photon. Res.*, vol. 2, no. 4, pp. B5–B10, Aug. 2014.

[8] W. Li and J. Yao, "Generation of linearly chirped microwave waveform with an increased time-bandwidth product based on a tunable optoelectronic oscillator," *J. Lightw. Technol.*, vol. 32, no. 20, pp. 3573–3579, Oct. 2014.

[9] Y. Zhang, X. Ye, Q. Guo, F. Zhang, and S. Pan, "Photonic generation of linear-frequency-modulated waveforms with improved time-bandwidth product based on polarization modulation," *J. Lightw. Technol.*, vol. 35, no. 10, pp. 1821–1829, May 2017.

[10] P. Zhou, F. Zhang, Q. Guo, and S. Pan, "Linearly chirped microwave waveform generation with large time-bandwidth product by optically injected semiconductor laser," *Opt. Express*, vol. 24, no. 16, pp. 18460–18467, Aug. 2016.

[11] S. C. Chan and J. M. Liu, "Tunable narrow-linewidth photonic microwave generation using semiconductor laser dynamics," *IEEE J. Sel. Topics Quantum Electron.*, vol. 10, no. 5, pp. 1025–1032, Sep. 2004.

[12] J. P. Zhuang, X. Z. Li, S. S. Li, and S. C. Chan, "Frequency-modulated microwave generation with feedback stabilization using an optically injected semiconductor laser," *Opt. Lett.*, vol. 41, no. 24, pp. 5784–5787, Dec. 2016.

[13] P. Zhou, F. Zhang, Q. Guo, and S. Pan, "Linear frequency-modulated waveform generation based on a tunable optoelectronic oscillator," in *Proc. 2017 IEEE Top. Meet. Microw. Photon.*, Beijing, China, Oct. 2017, paper Mo2.1.

[14] P. Zhou, F. Zhang, B. Gao, and S. Pan, "Optical pulse generation by an optoelectronic oscillator with optically injected semiconductor laser," *IEEE Photon. Technol. Lett.*, vol. 28, no. 17, pp. 1827–1830, Sep. 2016.

[15] X. S. Yao and L. Maleki, "Optoelectronic microwave oscillator," *J. Opt. Soc. Amer. B*, vol. 13, no. 8, pp. 1725–1735, Aug. 1996.

[16] P. Zhou, S. Pan, D. Zhu, R. Guo, F. Zhang, and Y. Zhao, "A compact optoelectronic oscillator based on an electroabsorption modulated laser," *IEEE Photon. Technol. Lett.*, vol. 26, no. 1, pp. 86–89, Jan. 2014.

[17] T. B. Simpson, J. M. Liu, K. F. Huang, and K. Tai, "Nonlinear dynamics induced by external optical injection in semiconductor lasers," *Quantum Semiclass. Opt.*, vol. 9, no. 5, pp. 765–784, May 1997.

[18] S. C. Chan, "Analysis of an optically injected semiconductor laser for microwave generation," *IEEE J. Quantum Electron.*, vol. 46, no. 3, pp. 421–428, Mar. 2010.

[19] S. K. Hwang, J. M. Liu, and J. K. White, "Characteristics of period-one oscillations in semiconductor lasers subject to optical injection," *IEEE J. Sel. Topics Quantum Electron.*, vol. 10, no. 5, pp. 974–981, Sep. 2004.

[20] M. Pochet, N. A. Naderi, Y. Li, V. Kovanis, and L. F. Lester, "Tunable photonic oscillators using optically injected quantum-dash diode lasers," *IEEE Photon. Technol. Lett.*, vol. 22, no. 11, pp. 763–765, Jun. 2010.

[21] R. Huber, M. Wojtkowski, and J. G. Fujimoto, "Fourier Domain Mode Locking (FDML): A new laser operating regime and applications for optical coherence tomography," *Opt. Express*, vol. 14, no. 8, pp. 3225–3237, Apr. 2006.

[22] F. Zhang, X. Ge, S. Pan, and J. Yao, "Photonics generation of pulsed microwave signals with tunable frequency and phase based on spectral shaping and frequency to time mapping," *Opt. Lett.*, vol. 38, no. 20, pp. 4256–4259, Oct. 2013.

[23] S. Pan, P. Zhou, Z. Tang, Y. Zhang, F. Zhang, and D. Zhu, "Optoelectronic oscillator based on polarization modulation," *Fiber Integr. Opt.*, vol. 34, no. 4, pp. 185–203, Oct. 2015.

[24] S. Pan and J. Yao, "A frequency-doubling optoelectronic oscillator using a polarization modulator," *IEEE Photon. Technol. Lett.*, vol. 21, no. 13, pp. 929–931, Jul. 2009.

[25] D. Zhu, S. Pan, and D. Ben, "Tunable frequency-quadrupling dual-loop optoelectronic oscillator," *IEEE Photon. Technol. Lett.*, vol. 24, no. 3, pp. 194–196, Feb. 2012.

[26] S. Pan and J. Yao, "Tunable subterahertz wave generation based on photonic frequency sextupling using a polarization modulator and a wavelength-fixed notch filter," *IEEE Trans. Microw. Theory Techn.*, vol. 58, no. 7, pp. 1967–1975, Jul. 2010.

[27] J. W. Shi, F. M. Kuo, N. W. Chen, S. Y. Set, C. B. Huang, and J. E. Bowers, "Photonic generation and wireless transmission of linearly/nonlinearly continuously tunable chirped millimeter-wave waveforms with high time-bandwidth product at W-band," *IEEE Photon. J.*, vol. 4, no. 1, pp. 215–223, Feb. 2012.

[28] O. C. Graydon, M. N. Zervas, and R. I. Laming, "Erbium-doped-fiber optical limiting amplifiers," *J. Lightw. Technol.*, vol. 13, no. 5, pp. 732–739, May 1995.

Pei Zhou (S'15) received the B.S. degree in electronic science and technology from Nanjing University of Aeronautics and Astronautics (NUAA), Nanjing, China, in 2013. He is currently working toward the Ph.D. degree at the Key Laboratory of Radar Imaging and Microwave Photonics (Nanjing Univ. Aeronaut. Astronaut.), Ministry of Education.

His current research interests include application of nonlinear laser dynamics, and microwave photonic signal generation.

Fangzheng Zhang (S'10–M'13) received the B.S. degree from Huazhong University of Science and Technology (HUST), Wuhan, China, and the Ph.D. degree from Beijing University of Posts and Telecommunications (BUPT), Beijing, China, in 2008 and 2013, respectively. He is currently with the College of Electronic and Information Engineering, Nanjing University of Aeronautics and Astronautics, as an Associate Professor.

His main research interests include microwave photonics, coherent optical communications, and all-optical signal processing.

Shilong Pan (S'06–M'09–SM'13) received the B.S. and Ph.D. degrees in electronics engineering from Tsinghua University, Beijing, China, in 2004 and 2008, respectively. From 2008 to 2010, he was a "Vision 2010" Postdoctoral Research Fellow in the Microwave Photonics Research Laboratory, University of Ottawa, Canada. In 2010, he joined the College of Electronic and Information Engineering, Nanjing University of Aeronautics and Astronautics, China, where he is currently a Full Professor and Deputy Director of the Key Laboratory of Radar Imaging and Microwave Photonics (Nanjing Univ. Aeronaut. Astronaut.), Ministry of Education.

His research has focused on microwave photonics, which includes optical generation and processing of microwave signals, analog photonic links, photonic microwave measurement, and integrated microwave photonics. He has authored or coauthored more than 360 research papers, including more than 190 papers in peer-reviewed journals and 170 papers in conference proceedings.

Prof. Pan is currently a Topical Editor of *Chinese Optics Letters*, and is a Technical Committee member of IEEE MTT-3 Microwave Photonics. He is a Steering Committee Member of IEEE International Topical Meeting on Microwave Photonics and International Conference on Optical Communications and Networks. Prof. Pan has also served as a Chair of a number of international conferences, symposia, and workshops, including the TPC Chair of the International Conference on Optical Communications and Networks in 2015, TPC Co-chair of IEEE International Topical Meeting on Microwave Photonics in 2017, TPC Subcommittee Chair or Co-chair of the IEEE Radio Wireless Symposium in 2013, 2014 and 2016, the OptoElectronics and Communication Conference in 2015, CLEO Pacific Rim in 2018, International Conference on Information Optics and Photonics in 2018, and Chair of the microwave photonics for broadband measurement workshop of International Microwave Symposium in 2015.

Prof. Pan is a senior member of the IEEE Microwave Theory and Techniques Society, the IEEE Photonics Society and the Optical Society of America. He was selected to receive an OSA outstanding reviewer award in 2015 and a top reviewer of IEEE/OSA Journal of Lightwave Technology in 2016. He was awarded the Excellent Young Scholars Award of the National Natural Science Foundation of China in 2014, and the Scientific and Technological Innovation Leading Talents Award of the National Ten Thousand Plan in 2018.